Nanoscale

Accepted Manuscript

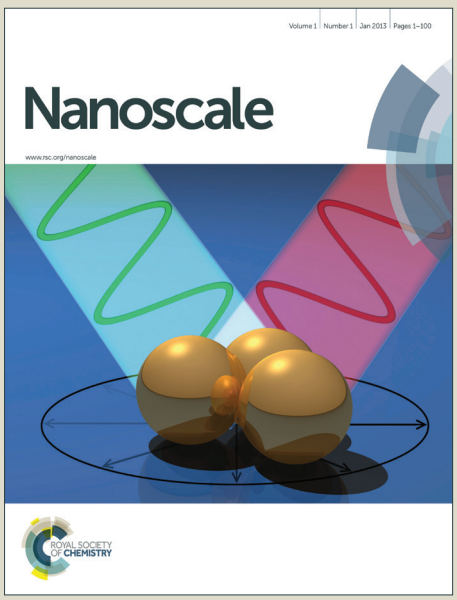

ROYAL SOCIETY OF CHEMISTRY

www.rsc.org/nanoscale

Engineering $Cu_2O/NiO/Cu_2MoS_4$ Hybrid Photocathode for H_2 Generation in Water

Chen Yang,[a,b] Phong D. Tran,[a,b] Pablo P. Boix,[b] Prince S. Bassi,[a] Natalia Yantara,[b] Lydia. H. Wong,[a*] James Barber[a,c]*

[a]*Solar Fuel Laboratory, School of Materials Science & Engineering, Nanyang Technological University, Singapore. Email: Lydia.wong@ntu.edu.sg*

[b]*Energy Research Institute @ Nanyang Technological University (ERI@N), Singapore. Email: dptran@ntu.edu.sg*

[c]*Division of Molecular Biosciences, Department of Life Sciences, Imperial College London, UK*

Abstract

We report a scalable process for fabricating a multiple-layer hybrid photocathode, namely $Cu_2O/NiO/Cu_2MoS_4$, for H_2 generation in water. In pH 5 solution and under 1 Sun illumination, the photocathode showed interesting photocatalytic properties. The onset photocurrent was recorded at +0.45 V *vs.* RHE while at 0 V *vs.* RHE, photocurrent density of 1.25 $mA.cm^{-2}$ was obtained. It was found that NiO interlayer enhances charge transfer from Cu_2O light harvester to Cu_2MoS_4 hydrogen evolution reaction electrocatalyst which in turn accelerates charge transfer at the electrode/ electrolyte interface and therefore improve photocatalytic properties of the Cu_2O photocathode.

Main Text

Solar-induced water splitting is considered as a promising technology to harvest abundant but intermitted solar energy and convert it into chemical energy stored within the H_2 molecule.[1,2] Recent theoretical calculation showed that solar-to-hydrogen conversion efficiencies up to 28-30% can be expected[3,4] that is just matching well with the US Department of Energy`s target. However, to achieve this efficiency, key challenges remain in searching for viable materials to engineer appropriate photoelectrodes which can be then assembled within a complete highly efficient bias-free photoelectrochemical cell (PEC).

$2H^+ + 2e^- \rightarrow H_2$ (eq. 1)

$Cu_2O + 2H^+ + 2e^- \rightarrow 2Cu + H_2O$ (eq. 2)

$2CuO + H_2O + 2e^- \rightarrow Cu_2O + 2OH^-$ (eq. 3)

Among available materials being considered for engineering photocathode, copper (I) oxide (Cu_2O) appears to be a promising candidate thanks to its visible light absorption properties (band gap of about 2.1 eV), abundance and its appropriate conduction band which provides sufficiently large reductive electrochemical potential upon illumination to drive the catalytic hydrogen evolution reaction (HER, *eq. 1*).[5] However, the main drawback of Cu_2O is its self-reduction (to Cu, *eq. 2*) and self-oxidation (to CuO, *eq. 3*) potentials lied within the band gap.[5] To limit the self-reduction process, it is critical to drive photo-generated electrons to Cu_2O electrode surface and use these electrons for the HER in an efficient manner.[5,6] Due to the low kinetic of the HER on the pristine Cu_2O electrode surface, employing an HER electrocatalyst as co-catalyst is needed.[1,2,7]

Indeed, the best electrocatalyst for the HER is platinum, which is therefore a judicious choice of co-catalyst for constructing hybrid photocathode for the H_2 generation.[5] However, employing platinum or other precious elements may not be the most economical solution to realize cost-effective photoelectrodes/ photoelectrochemical cells. Moreover, unlike low conduction band semiconductors e.g. TiO_2 (E_{CB} = -0.17V *vs.* RHE (*Reversible Hydrogen Electrode*)) wherein using an extremely active electrocatalyst functioning with very low overpotential e.g. Pt (η ~30mV) is needed, a larger choice of HER co-catalysts can be applied for semiconductors having more reductive conduction band such as Si, CdS.[8-12] Cu_2O has conduction band positioned at potential about -0.7 V *vs.* RHE.[13] Hence, in principle

numerous HER electrocatalysts can be used as co-catalyst to promote the H_2 generation on Cu_2O surface electrode.

Recently, sulfides of transition metals e.g. $(Mo/W)(S/Se)_2$, Co(S/Se) have gained great attention as low-cost, potential electrocatalysts for the H_2 generation in water.[14-19] Employing MoS_2 co-catalyst to enhance photocatalytic activities of diverse semiconducting photocatalysts/ photoelectrodes has been described.[8-10,20,21] We have demonstrated hetero-bimetallic sulfides as promising electrocatalysts for the HER in water over wide pH range (pH 0- 12) with very good stability and relatively low overpotential requirement of about 130- 150 mV.[18,19] Herein, we report on using of nanopowder copper-molybdenum-sulfide (Cu_2MoS_4) co-catalyst to promote the H_2 photo-generation on Cu_2O photocathode in water. We found that Cu_2MoS_4 co-catalyst induced a significant anodic shift of 300 mV of onset potential, together with a significant improved photostability of Cu_2O photocathode.

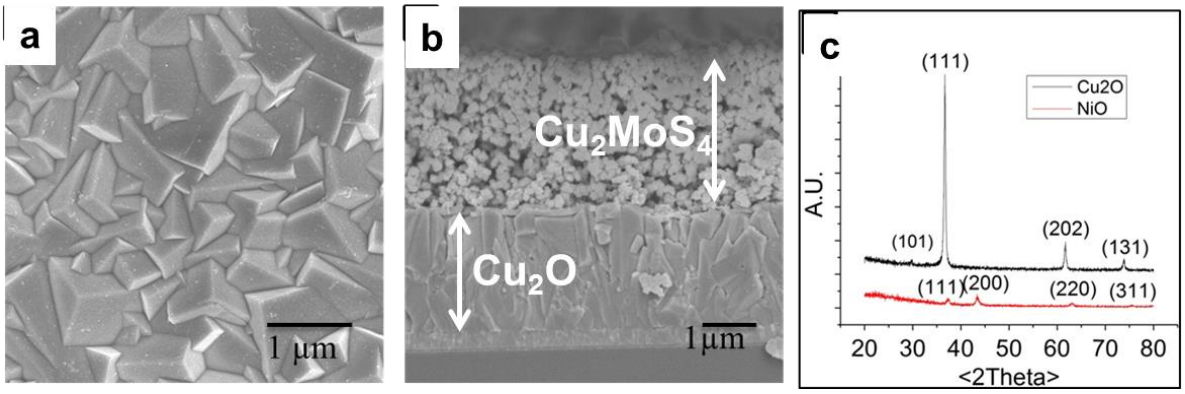

Figure 1: *Characterization of as-deposited Cu_2O and hybrid multiple-layer $Cu_2O/NiO/Cu_2MoS_4$ electrodes.* ***a****) SEM image (top view) of a pristine Cu_2O electrode.* ***b****) Cross section analysis of a $Cu_2O/NiO/Cu_2MoS_4$ photoelectrode. The NiO interlayer is not visible.* ***c****) XRD patterns of Cu_2O (black) and NiO (red) deposited on FTO substrate.*

Cu_2O photoactive thin film (thickness of ~2.3 µm) was electrodeposited on clean conductive fluorine-doped tin oxide (FTO) substrate employing an alkaline copper lactate solution, following the preparation process reported by Golden *et al.*[22] SEM analysis showed compact morphology with relatively large Cu_2O grains (**figures 1a, S1**) while XRD analysis revealed crystalline Cu_2O structure with Cu_2O (111) dominant phase (**figure 1c**). The photoelectrochemical properties of the deposited Cu_2O electrode were then evaluated in a pH

5 Na_2SO_4 (1M) solution buffered with $NaHSO_4$. A three-electrode-configuration electrochemical cell was employed. The counter electrode was a Pt wire while the reference electrode was an Ag/AgCl 3M KCl. All potential was quoted versus the Reversible Hydrogen Electrode (RHE). Cu_2O working electrode having photoactive area of $0.23cm^2$ was illuminated with standard 1 Sun light source. We adopted back side (FTO side) illumination configuration in order to simulate the best function of the Cu_2O-based photocathode in perspective of assembling this photocathode together with an appropriate photoanode to engineer a complete Z-scheme photoelectrochemical cell. Indeed, in a Z-scheme cell, light is expected to illuminate on the photoanode front-site.

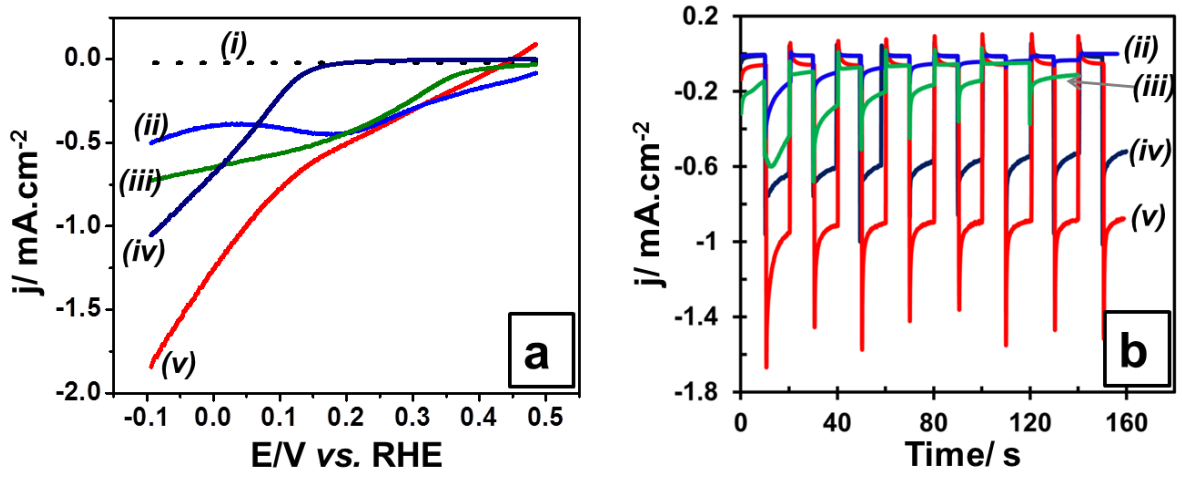

Figure 2: *Photoelectrochemical properties of Cu_2O-based photocathodes in a pH5 Na_2SO_4 (1M) solution.* ***a****) I-V curves collected under 1 Sun illumination on a pristine Cu_2O (curve (**ii**)), a Cu_2O/ Cu_2MoS_4 (curve (**iii**)), a Cu_2O/ NiO (curve (**iv**)) and a Cu_2O/ NiO/ Cu_2MoS_4 (curve (**v**)) photocathode. Without light illumination, these Cu_2O-based photocathodes showed similar I-V curves. For clarification, only the curve collected on a Cu_2O/NiO/Cu_2MoS_4 (curve (**i**) was presented.* ***b****) Generated photocurrent achieved at applied potential of 0V vs. RHE employing a pristine Cu_2O (curve (**ii**)), Cu_2O/Cu_2MoS_4 (**iii**), Cu_2O/NiO (curve (**iv**), and a Cu_2O/NiO/Cu_2MoS_4 (curve (**v**)) photocathode.*

As presented in **figure 2a** (curve (***ii***)), the pristine Cu_2O photoelectrode showed important photocurrent even at low applied bias, from 0 to +0.5 V *vs.* RHE. In this potential range, a current peak at ca. +0.25 V *vs.* RHE was observed. Similar phenomenon was found for other

Cu_2O photoelectrodes which showed a photocurrent peak at ca. +0.3 V *vs.* RHE as reported by Paracchino *et al.*[23] We note that Parrachino *et al.* deployed photogenerated current in this positive potential range to quantify the photocatalytic activities of electrodeposited Cu_2O photoelectrodes. Indeed, the photogenerated currents at potentials more positive than 0 V *vs.* RHE are of great interests in the context of application for the solar-hydrogen production if and only if these currents are relevant to the photo-reduction of proton into hydrogen. However, photoelectrolysis at +0.25V *vs.* RHE employing a 1.5 cm^2 Cu_2O photoelectrode in a gas-tight closed electrochemical cell showed almost no photogeneration of hydrogen gas as analysed by gas chromatography. Photocurrent-to-hydrogen yield of only 0.54% (**figure S2**) was calculated for 10 min continuous measurement under 1 Sun illumination. It is consistent with Electrochemical Impedance Spectroscopy (EIS) analysis. Nyquist plot analysis for an illuminated Cu_2O electrode hold at +0.3V *vs.* RHE showed no charge transfer at the Cu_2O/electrolyte interface (**figure 3,** curve ***(ii)***). XRD analysis performed on the Cu_2O electrode after photoelectrolysis experiment showed the appearance of Cu metal peaks (**figure S3**). Therefore, we conclude the photocurrent observed is originated from the self-reduction of Cu_2O into Cu metal. Similar zero current-to-H_2 yield was recorded by Lin *et al* for a Cu_2O nanowires electrode at less positive potential of 0V *vs.* RHE in a pH 6 Na_2SO_4 solution.[24]

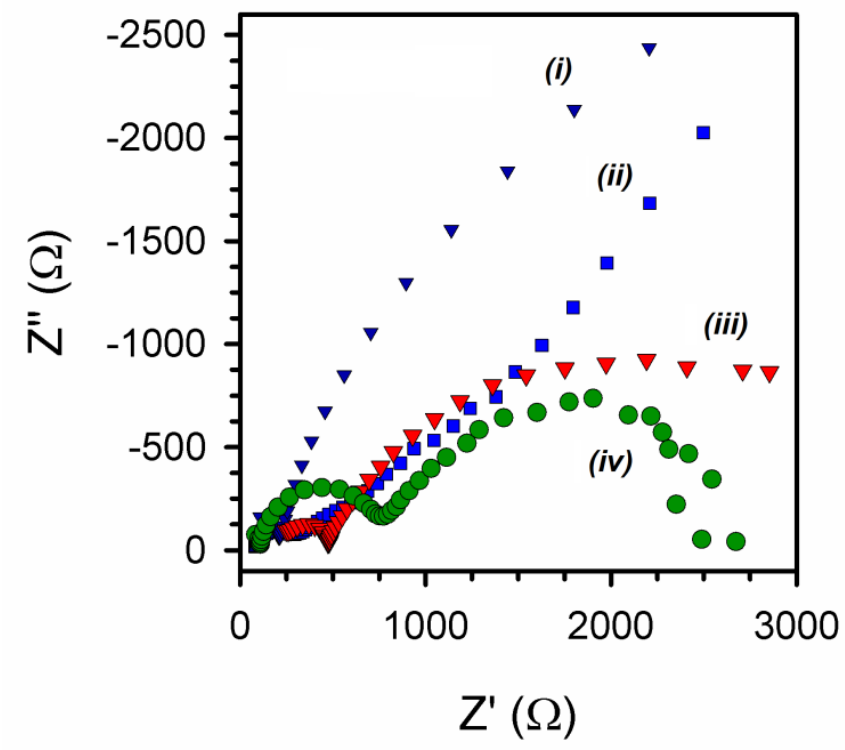

Figure 3: *Nyquist plots analysis performed on Cu_2O-based photoelectrodes immersed in a pH5 Na_2SO_4 (1M) solution, at applied bias of +0.3V vs. RHE, under illumination: Cu_2O/ NiO (curve (**i**)), Pristine Cu_2O (curve (**ii**)), Cu_2O/NiO/Cu_2MoS_4 (curve (**iii**)) and Cu_2O/Cu_2MoS_4 (curve (**iv**)).*

A layer of Cu_2MoS_4 HER electrocatalyst (thickness of ~2.7 µm) was then deposited on surface of the Cu_2O electrode, employing a scalable solution process in order to enhance the kinetic of the HER at the Cu_2O/ electrolyte interface (**figure 1b**). To do so, a well-dispersed suspension of Cu_2MoS_4 nanopowder in water was drop-casted on Cu_2O electrode surface, followed by air-drying prior to characterizations. It is worth noting that a back-side illumination on the Cu_2O electrodes allows removing visible light absorption effect of the Cu_2MoS_4 layer decorated. It was found that the Cu_2MoS_4 strongly absorbs visible light but displays negligible photocatalytic activities (**figures S4, S5**). EIS analysis showed enhanced charge transfer at the Cu_2O/Cu_2MoS_4 electrode surface interfaced with electrolyte solution compared with that observed for the pristine Cu_2O/ electrolyte interface, thus clearly evidenced the electrocatalytic role of the deposited Cu_2MoS_4 layer (**figure 3**, curves (***ii***) and (***iv***)). Nyquist plot collected at potential +0.3V *vs.* RHE on the illuminated Cu_2O/Cu_2MoS_4 displayed two semicircles. We attributed the first semicircle to the electron transfer from Cu_2O conduction band to Cu_2MoS_4 electrocatalyst while the second semicircle is attributed to the electron injection from Cu_2MoS_4 to the electrolyte, which induces the H_2 evolution. However, the Cu_2O/Cu_2MoS_4 electrode showed low photostability. The photogenerated current was found to rapidly decrease with time, as observed for a pristine Cu_2O electrode without Cu_2MoS_4 co-catalyst decoration (**figure 2b**, curves (***ii***) and (***iii***)). We tentatively attribute this instability to the fact that the porosity of the Cu_2MoS_4 layer is permeable to protons that causes the photocorrosion of Cu_2O (*eq. 2*). It suggests that a more efficient protective layer placed in between Cu_2O light harvester and Cu_2MoS_4 electrocatalyst layer is required.

For such interlayer purpose, we have chosen NiO material. Indeed, NiO has a large band gap of about 3.6 eV and thus does not absorb visible light.[25] It has been shown to be an effective protective layer for Cu_2O nanowires photocathode.[24] We deposited NiO layer on Cu_2O electrode surface employing method described by Lin *et al*[24] with some slight modification (*refer SI for details*). The thickness of NiO layer was controlled by varying number of deposition cycles (N= 1-5). Each NiO deposition cycle refers to spin-coating a volume of 50

µL solution of 0.5M $Ni(OAc)_2$ precursor in 2-methoxyethanol onto geometrical 2.25cm^2 Cu_2O electrode, followed by annealing at 220℃ in air for 30 min. Elemental analysis performed on a Cu_2O/ NiO (N=2) by Energy Dispersive X-ray Spectroscopy (EDX) showed Cu, O and Ni elements (**figure S6**), thus suggesting production of NiO layer on Cu_2O surface after above treatment with $Ni(OAc)_2$ precursor. However, attempts to quantify the thickness of deposited NiO layer on Cu_2O via SEM cross section analysis were unsuccessful, likely due to the rough Cu_2O electrode surface and the thin NiO layer. To overcome this problem and make sure the deposited material from $Ni(OAc)_2$ precursor was indeed the expected NiO, we performed control deposition on smooth FTO substrate. NiO film with a thickness of 156 nm was deposited by repeating 10 deposition cycles (N=10) (**figure S7)**. XRD analysis of this film clearly confirmed deposition of crystalline NiO (**figure 1c**). Assuming a uniform growth, an average growth rate was estimated to be around 16 nm per deposition cycle.

We then aimed to optimize the thickness required for the NiO to protect the Cu_2O photoelectrode. As shown in **figures 2a and S8**, the photocurrent peak at +0.25V *vs.* RHE corresponding to the photocorrosion of Cu_2O was decreased upon depositing one cycle of NiO (~16nm thickness). The best protective effect was achieved after 2 cycles of NiO treatment. The obtained Cu_2O/ NiO (~32nm) displayed onset potential at +0.15V *vs.* RHE for the photocurrent generation. Cu_2O treated with thicker NiO film showed slightly lower photogenerated current even the same onset potential was recorded. That is likely due to the low conductivity of thick NiO film. As further illustration, photoelectrolysis at 0 V *vs.* RHE under 1 Sun illumination employing an untreated Cu_2O photocathode showed a fast decreased photocurrent (**figure 2b**, curve (***ii***)), while significantly more stable photocurrent was recorded for a Cu_2O/NiO (~32nm) photocathode (**figure 2b**, curve (***iv***)).

Decorating Cu_2MoS_4 electrocatalyst on Cu_2O/NiO (~32nm) electrode benefits from the stability improvement achieved with the NiO layer, resulting in further significant improvement of photoelectrochemical properties. An onset photocurrent shifting to anodic direction of 0.3V was recorded with employing Cu_2MoS_4 electrocatalyst (**figure 2a, curve (*v*)** *versus* curve **(*iv*)**). That is thus among the most effective potential shifting ever recorded for an electrocatalyst decorated on a photocathode surface.[5,8,26] We note that for the purpose of engineering a complete Z-scheme photoelectrochemical cell for solar-induced water splitting by assembling appropriate photoanode and photocathode, each value of onset potential shifting to anodic direction for the photocathode and to cathodic direction for the photoanode is valuable. The hybrid photocathode Cu_2O/NiO/Cu_2MoS_4 displayed onset photocurrent

potential at +0.45V *vs.* RHE, thus comparable to that reported by Parrachino et al. for the multiple-layers $Cu_2O/ZnO/TiO_2/Pt$ photocathode.[5,23] At constant holding potentials of 0V and +0.3V *vs*. RHE, our $Cu_2O/NiO/Cu_2MoS_4$ photocathode generated stable photocurrent, suggesting a good photostability (**figures 2b and S9**). These generated cathodic photocurrents have origin from the light harvesting properties of the Cu_2O absorber since control experiments performed under identic conditions employing a NiO/Cu_2MoS_4 photoelectrode showed negligible anodic photocurrent (**figure S5**). Furthermore, in very sharp contrast with the case of pristine Cu_2O discussed above, photocurrent generated on the $Cu_2O/NiO/Cu_2MoS_4$ photocathode at +0.3V *vs.* RHE has important contribution from the photoreduction of proton into H_2. Photocurrent-to-H_2 yield of about 31.2% was calculated for this case, on basis of 10 min photoelectrolysis. This performance is also higher than that achieved when employing a Cu_2O/NiO (N=2) photocathode without decorating Cu_2MoS_4 co-catalyst. At applied potential of 0V *vs.* RHE, faradic current efficiency of 23.1% was calculated (**figure S2**). We note that these current efficiencies are close to that previously reported by Lin *et al*. for a Cu_2O/NiO photocathode in pH 6 solution (at E_{appl} = 0V *vs.* RHE, faradic efficiency of 32±6% was calculated on basis of 15 min photoelectrolysis).[24] However, bulk photo-electrolysis for longer time showed decreased Faradic current efficiency (**figure S2**). It indicates photocorrosion process still occurred together with the H_2 evolution when the current Cu_2O-based photocathodes are used.

Even though the NiO interlayer was not able to totally suppress the photocorrosion of Cu_2O, its positive contribution to improve the photostability and photocatalytic activities of the Cu_2O photocathode was clearly evidenced. EIS analysis explains the role of NiO interlayer on performance improvement. The lower frequency arc obtained in the Nyquist plot, which is attributed to the charge transfer from the Cu_2MoS_4 to the solution, is not significantly affected by the NiO interlayer: similar arc resistances are obtained in the fitting of both Cu_2O/Cu_2MoS_4 (2617 Ω) and $Cu_2O/NiO/Cu_2MoS_4$ systems (2781 Ω) as seen in **figure S10 and table S1**. However, the interlayer of NiO diminishes the higher frequency arc (651 Ω for Cu_2O/Cu_2MoS_4 and 211 Ω for $Cu_2O/NiO/Cu_2MoS_4$), which indicates a better charge injection from Cu_2O to Cu_2MoS_4. This improvement has probably its origin in the energetic tuning of the interface: the p-type doping properties of the deposited NiO thin layer revealed by X-ray photoelectron spectroscopy (XPS) (**figure S11**) can modify the band alignment, generating a favourable band bending for the charge injection. Similar effects have been

reported in other kind of devices where thin layers of NiO improved the electrical behavior of the interfaces despite its low conductivity.[27]

To sum up, we reported herein scalable fabrication of a promising hybrid photocathode for solar-induced H_2 generation in water. The photoelectrode $Cu_2O/NiO/Cu_2MoS_4$ was made of only earth-abundant-elements and thus represents an attractive example of noble-metal free photocatalytic material. The NiO interlayer was found to enhance charge transfer from light harvester Cu_2O to Cu_2MoS_4 electrocatalyst whose incorporation accelerates charge transfer cross photoelectrode/ electrolyte interface and therefore enhances the photocatalytic activities of Cu_2O for the H_2 generation. Spin coating method adopted in this work can be also easily applied to incorporate NiO interlayer and Cu_2MoS_4 electrocatalytic layer in other photocathode systems.

We note that our hybrid photocathode $Cu_2O/NiO/Cu_2MoS_4$ is still less effective than the best copper-based multiple-layers photocathode reported by Paracchino et al.[5] At 0V *vs.* RHE, a photocurrent of ~1.25 $mA.cm^{-2}$ was recorded for the Cu_2O/NiO (32 nm)/Cu_2MoS_4 photocathode which is about 6 times lower than that achieved for the $Cu_2O/ZnO/TiO_2/Pt$ photocathode under similar conditions. We tentatively attribute this to lower photoelectrochemical properties of our bare Cu_2O electrode compared with the bare electrode employed by Paracchino et al (0.37$mA.cm^{-2}$ compared with 2.5mA at E_{appl} of +0.3V vs. RHE). We can therefore expect higher performance of the hybrid photocathode once the photoelectrochemical properties of our bare Cu_2O are improved.

Acknowledgments

CY acknowledges Energy Research Institute @ Nanyang Technological University for PhD scholarship. TDP, LHW and JB acknowledge the Centre for Artificial Photosynthesis (CAP) at NTU for facilities support.

References and Notes

1 Tran, P. D., Wong, L. H., Barber, J. & Loo, J. S. C. Recent advances in hybrid photocatalysts for solar fuel production. *Energy & Environmental Science* **5**, 5902, doi:10.1039/c2ee02849b (2012).

2 Barber, J. & Tran, P. D. From natural to artificial photosynthesis. *Journal of the Royal Society, Interface / the Royal Society* **10**, 20120984, doi:10.1098/rsif.2012.0984 (2013).

3 Winkler, M. T., Cox, C. R., Nocera, D. G. & Buonassisi, T. Modeling integrated photovoltaic–electrochemical devices using steady-state equivalent circuits. *Proceedings of the National Academy of Sciences* **110**, E1076-E1082, doi:10.1073/pnas.1301532110 (2013).

4 Hu, S., Xiang, C., Haussener, S., Berger, A. D. & Lewis, N. S. An analysis of the optimal band gaps of light absorbers in integrated tandem photoelectrochemical water-splitting systems. *Energy & Environmental Science* **6**, 2984-2993, doi:10.1039/C3EE40453F (2013).

5 Paracchino, A., Laporte, V., Sivula, K., Gratzel, M. & Thimsen, E. Highly active oxide photocathode for photoelectrochemical water reduction. *Nat Mater* **10**, 456-461, doi:10.1038/nmat3017 (2011).

6 Tran, P. D. *et al.* A cuprous oxide-reduced graphene oxide (Cu2O-rGO) composite photocatalyst for hydrogen generation: employing rGO as an electron acceptor to enhance the photocatalytic activity and stability of Cu2O. *Nanoscale* **4**, 3875-3878, doi:10.1039/c2nr30881a (2012).

7 Walter, M. G. *et al.* Solar Water Splitting Cells. *Chemical Reviews* **110**, 6446-6473, doi:10.1021/cr1002326 (2010).

8 Tran, P. D. *et al.* Novel assembly of an MoS2 electrocatalyst onto a silicon nanowire array electrode to construct a photocathode composed of elements abundant on the earth for hydrogen generation. *Chemistry- A European Journal* **18**, 13994-13999, doi:10.1002/chem.201202214 (2012).

9 Nguyen, M. *et al.* In situ photo-assisted deposition of MoS(2) electrocatalyst onto zinc cadmium sulphide nanoparticle surfaces to construct an efficient photocatalyst for hydrogen generation. *Nanoscale* **5**, 1479-1482, doi:10.1039/c2nr34037b (2013).

10 Seger, B. *et al.* Hydrogen Production Using a Molybdenum Sulfide Catalyst on a Titanium-Protected n+p-Silicon Photocathode. *Angewandte Chemie International Edition* **51**, 9128-9131, doi:10.1002/anie.201203585 (2012).

11 Krawicz, A. *et al.* Photofunctional construct that interfaces molecular cobalt-based catalysts for H2 production to a visible-light-absorbing semiconductor. *Journal of the American Chemical Society* **135**, 11861-11868, doi:10.1021/ja404158r (2013).

12 Zong, X. *et al.* Photocatalytic H2 Evolution on CdS Loaded with WS2 as Cocatalyst under Visible Light Irradiation. *The Journal of Physical Chemistry C* **115**, 12202-12208, doi:10.1021/jp2006777 (2011).

13 de Jongh, P. E., Vanmaekelbergh, D. & Kelly, J. J. Photoelectrochemistry of Electrodeposited Cu2 O *Journal of The Electrochemical Society* **147**, 486-489, doi:10.1149/1.1393221 (2000).

14 Jaramillo, T. F. *et al.* Identification of Active Edge Sites for Electrochemical H2 Evolution from MoS2 Nanocatalysts. *Science* **317**, 100-102, doi:10.1126/science.1141483 (2007).

15 Voiry, D. *et al.* Enhanced catalytic activity in strained chemically exfoliated WS2 nanosheets for hydrogen evolution. *Nat Mater* **12**, 850-855, doi:10.1038/nmat3700 (2013).

16 Sun, Y. *et al.* Electrodeposited Cobalt-Sulfide Catalyst for Electrochemical and Photoelectrochemical Hydrogen Generation from Water. *Journal of the American Chemical Society* **135**, 17699-17702, doi:10.1021/ja4094764 (2013).

17 Kong, D. *et al.* Synthesis of MoS2 and MoSe2 Films with Vertically Aligned Layers. *Nano letters* **13**, 1341-1347, doi:10.1021/nl400258t (2013).

18 Tran, P. D. *et al.* Copper molybdenum sulfide: a new efficient electrocatalyst for hydrogen production from water. *Energy & Environmental Science* **5**, 8912, doi:10.1039/c2ee22611a (2012).

19 Tran, P. D. *et al.* Novel cobalt/nickel–tungsten-sulfide catalysts for electrocatalytic hydrogen generation from water. *Energy & Environmental Science* **6**, 2452, doi:10.1039/c3ee40600h (2013).

20 Zong, X. *et al.* Enhancement of Photocatalytic H2 Evolution on CdS by Loading MoS2 as Cocatalyst under Visible Light Irradiation. *Journal of the American Chemical Society* **130**, 7176-7177, doi:10.1021/ja8007825 (2008).

21 Morales-Guio, C. G., Tilley, S. D., Vrubel, H., Gratzel, M. & Hu, X. Hydrogen evolution from a copper(I) oxide photocathode coated with an amorphous molybdenum sulphide catalyst. *Nature communications* **5**, 3059, doi:10.1038/ncomms4059 (2014).

22 Golden, T. D. *et al.* Electrochemical Deposition of Copper(I) Oxide Films. *Chemistry of Materials* **8**, 2499-2504, doi:10.1021/cm9602095 (1996).

23 Paracchino, A., Brauer, J. C., Moser, J.-E., Thimsen, E. & Graetzel, M. Synthesis and Characterization of High-Photoactivity Electrodeposited Cu2O Solar Absorber by Photoelectrochemistry and Ultrafast Spectroscopy. *The Journal of Physical Chemistry C* **116**, 7341-7350, doi:10.1021/jp301176y (2012).

24 Lin, C.-Y., Lai, Y.-H., Mersch, D. & Reisner, E. Cu2O|NiOx nanocomposite as an inexpensive photocathode in photoelectrochemical water splitting. *Chemical Science* **3**, 3482, doi:10.1039/c2sc20874a (2012).

25 Miseki, Y., Kato, H. & Kudo, A. Water splitting into H2 and O2 over niobate and titanate photocatalysts with (111) plane-type layered perovskite structure. *Energy & Environmental Science* **2**, 306-314, doi:10.1039/B818922F (2009).

26 Oh, I., Kye, J. & Hwang, S. Enhanced Photoelectrochemical Hydrogen Production from Silicon Nanowire Array Photocathode. *Nano letters* **12**, 298-302, doi:10.1021/nl203564s (2011).

27 Ripolles-Sanchis, T., Guerrero, A., Azaceta, E., Tena-Zaera, R. & Garcia-Belmonte, G. Electrodeposited NiO anode interlayers: Enhancement of the charge carrier selectivity in organic solar cells. *Solar Energy Materials and Solar Cells* **117**, 564-568, doi:http://dx.doi.org/10.1016/j.solmat.2013.07.020 (2013).